In-plane paraconductivity in $La_{2-x}Sr_xCuO_4$ thin film superconductors at high reduced temperatures: Independence of the normal-state pseudogap

Severiano R. Currás,[1,2,*] Gonzalo Ferro,[1] M. Teresa González,[1] Manuel V. Ramallo,[1] Mauricio Ruibal,[1] José Antonio Veira,[1] Patrick Wagner,[1,2,†] and Félix Vidal[1,‡]

[1]*Laboratorio de Baixas Temperaturas e Superconductividade,[§] Departamento de Física da Materia Condensada, Universidade de Santiago de Compostela, E15782 Santiago de Compostela, Spain*

[2]*Laboratorium voor Vaste-Stoffysica en Magnetisme, Katholieke Universiteit Leuven, Celestijnenlaan 200 D, B3001 Heverlee, Belgium*

(Received 24 September 2002; revised manuscript received 28 May 2003; published 3 September 2003)

The in-plane resistivity has been measured in $La_{2-x}Sr_xCuO_4$ (LSCO) superconducting thin films of underdoped ($x=0.10,0.12$), optimally doped ($x=0.15$), and overdoped ($x=0.20,0.25$) compositions. These films were grown on (100)$SrTiO_3$ substrates, and have about 150 nm thickness. The in-plane conductivity induced by superconducting fluctuations above the superconducting transition (the so-called in-plane paraconductivity $\Delta\sigma_{ab}$) was extracted from these data in the reduced-temperature range $10^{-2}\lesssim\varepsilon\equiv\ln(T/T_c)\lesssim 1$. This $\Delta\sigma_{ab}(\varepsilon)$ was then analyzed in terms of the mean-field-like Gaussian-Ginzburg-Landau (GGL) approach extended to the high-ε region by means of the introduction of a total-energy cutoff, which takes into account both the kinetic energy and the quantum localization energy of each fluctuating mode. The obtained GGL coherence length amplitude in the c direction, $\xi_c(0)$, is constant for $0.10\leqslant x\leqslant 0.15$ [$\xi_c(0)\simeq 0.9$ Å], and decreases with increasing x in the overdoped range [$\xi_c(0)\simeq 0.5$ Å for $x=0.20$ and $\xi_c(0)\sim 0$ Å for $x=0.25$]. These results strongly suggest, therefore, that the superconducting fluctuations in underdoped and overdoped LSCO thin films may still be described, as in the optimally doped cuprates, in terms of the extended GGL approach; the main effect of doping is simply to change the fluctuations' dimensionality by varying the transversal superconducting coherence length amplitude. In contrast, the total-energy cutoff amplitude ε^c remains unchanged well within the experimental uncertainties. Our results strongly suggest that at all temperatures above T_c, including the high reduced-temperature region, doping mainly affects the normal-state properties in LSCO thin films and that its influence on the superconducting fluctuations is relatively moderate; even in the high-ε region, the in-plane paraconductivity is found to be independent of the opening of a pseudogap in the normal state of the underdoped films. We expect this last conclusion to be independent of the structural details of our films, i.e., applicable also to bulk samples.

DOI: 10.1103/PhysRevB.68.094501 PACS number(s): 74.25.Fy, 74.72.Dn, 74.40.+k

I. INTRODUCTION

It is well established that some of the most core properties of high-temperature cuprate superconductors (HTSC) strongly depend on hole doping.[1] These properties include, e.g., the normal-superconducting transition temperature T_c and the opening of a pseudogap in the normal region in underdoped cuprates. Another property much affected by doping is the in-plane electrical conductivity parallel to the CuO_2 planes, σ_{ab}, above the normal-superconducting transition.[1] It is also known that σ_{ab} in any HTSC is strongly affected around T_c by the presence of evanescent Cooper pairs created by thermal fluctuations (the so-called in-plane paraconductivity $\Delta\sigma_{ab}$).[2,3] In fact, these fluctuation effects may be appreciable even as far above T_c as $T\simeq 1.5T_c$. So, σ_{ab} may be decomposed as

$$\sigma_{ab}(T,x)=\Delta\sigma_{ab}(T,x)+\sigma_{abB}(T,x), \tag{1}$$

where T is the temperature, x is the hole doping level, and $\sigma_{abB}(T,x)$ is the so-called background or bare electrical in-plane conductivity (i.e., the electrical in-plane conductivity if the fluctuations are absent). It is then natural to ask how much of the variation of $\sigma_{ab}(T,x)$ observed when the doping is changed is due to $\Delta\sigma_{ab}(T,x)$, and how much to $\sigma_{abB}(T,x)$. In fact, once $\sigma_{ab}(T,x)$ is measured, the above question is equivalent to asking how $\Delta\sigma_{ab}(T,x)$ is affected by doping. This last question was first addressed by Suzuki and Hikita[4] and by Cooper *et al.*,[5] and since then by different authors.[6–14] However, as of today some of the main conclusions (including, e.g., the dimensionality of the fluctuations or the influence of the normal-state pseudogap) are still not well settled or are even contradictory. For instance, in the case of $YBa_2Cu_3O_x$ (YBCO), some authors[5,8,13] proposed that $\Delta\sigma_{ab}$ becomes more three dimensional (3D) when x increases, whereas other authors[6,11] did not find any appreciable dimensionality variation. Also, other authors have proposed, by analyzing either the fluctuation magnetization[14] or the thermal expansion,[12] that the superconducting fluctuations in underdoped YBCO do not follow the Gaussian mean-field-like theories used in Refs. 5,6,8,11,13 but instead different forms of non-Gaussian fluctuations.[12,14] Another example of these discrepancies is provided by the studies of $La_{2-x}Sr_xCuO_4$ (LSCO): by analyzing their measurements of the in-plane conductivity and magnetoconductivity, Suzuki and Hikita[4] proposed a change in dimensionality (from 2D to 3D) as doping increases from underdoped ($x<0.15$) to overdoped ($x>0.15$). In contrast, other authors[7] do not observe such a doping dependence in their magnetoresistance measurements in the same compounds. Let us stress here again that in addition to their interest for understanding the super-

conducting fluctuations in HTSC, the dependence of the paraconductivity on the doping may also concern other as yet unresolved problems, such as the origin of the pseudogap which opens in the normal state in the underdoped HTSC.[1] For instance, various theoretical models for this pseudogap (see, e.g., Refs. 15–17) predict that the fluctuation effects would strongly vary with the doping level (and even change their order of magnitude), while in other models (see, e.g., Refs. 18–21) the pseudogap does not result in a change in the superconducting fluctuations.

Among the various possible reasons for the above-commented discrepancies between different studies of $\Delta\sigma_{ab}(T,x)$, four of them seem to be predominant: first, the different structural characteristics of the samples studied by each author (bulk or film samples, and in the latter case their thickness and substrate lattice parameters). In particular, as it is now well established,[22–26] the substrate effects (including the associated strain effects) change some of the properties of these thin films, such as the absolute values of their T_c and in-plane normal resistivity. The ''fine'' details of the paraconductivity, such as its dimensionality (which is directly related to the superconducting coherence length amplitude in the c direction), may also depend on the structural nature of the samples. However, it is currently accepted that the most general aspects of HTSC are similar for both bulk and thin film samples. This is the case, in particular, of the evolution of T_c with doping or the appearance in the underdoped compositions of a pseudogap in the normal state.[1,4,5,7,23,24,26] Therefore, the conclusions concerning the relationships between superconducting fluctuations and pseudogap effects, or the existence or not of indirect paraconductivity effects (see below), may be expected to be general, i.e., independent of the superconductor's structural characteristics. A second source of ambiguity is the probable presence in some of the samples of structural and stoichiometric inhomogeneities which, even when they are relatively small, may appreciably affect the measured $\sigma_{ab}(T,x)$, mainly near T_c.[27] Third, some authors[4,11] analyze their $\Delta\sigma_{ab}(T,x)$ data in terms of the direct Aslamazov-Larkin (AL) contributions plus a pair-breaking Maki-Thompson (MT) term, while others[6,8–10,13] take into account only the AL contributions, and others still[5,7] opt for neither one possibility nor the other. Finally, a fourth source of ambiguity is that the region of reduced temperatures, $\varepsilon \equiv \ln(T/T_c)$, where the data were analyzed, was relatively small, typically $10^{-2} \lesssim \varepsilon \lesssim 0.1$, due to the fact that the conventional GGL approach is not applicable either very close to or very far from T_c.[2,3] To analyze the region $\varepsilon \gtrsim 0.1$, the usual mean-field-like theories have to be extended to deal with short-wavelength fluctuations, which above T_c become particularly important when the superconducting coherence length $\xi(T)$ falls in the range of its amplitude extrapolated to zero temperature, $\xi(0)$.[2] Various attempts to study the paraconductivity in the high-ε region as a function of doping in HTSC have been recently made by different authors.[9,10,13] In particular, Leridon *et al.*[13] analyzed the high-ε paraconductivity in YBCO thin films with different dopings. However, these authors based their analyses on a purely heuristic expression for the high-ε paraconductivity, so that the physical meaning of the involved parameters remains unclear. The high-ε paraconductivity as a function of doping in $Bi_2Sr_2CaCu_2O_{8+x}$ has been studied by Asaka *et al.*[9] (using Ge-doped crystals) and Silva *et al.*[10] (using oxygen-doped crystals but only in the overdoped range). These authors analyzed their data in terms of the GGL approach with the conventional kinetic energy (also called momentum) cutoff. Unfortunately, this conventional cutoff[2] extends the applicability of the GGL paraconductivity only up to approximately $\varepsilon \simeq 0.2$. Both groups find that the cutoff parameter is doping dependent, which Asaka *et al.* have attributed to variations in the in-plane coherence length amplitude $\xi_{ab}(0)$ and Silva *et al.* to possible deviations from the BCS theory.

To further clarify the effects of doping near T_c on the superconducting fluctuations in HTSC, in this work we measure and analyze the in-plane paraconductivity of different high-quality LSCO thin films with a thickness of ~ 150 nm, grown on $(100)SrTiO_3$ substrates, with a Sr content corresponding to $x = 0.10$, 0.12, 0.15, 0.20, and 0.25. These kinds of samples allow us to compare even the ''fine'' details of the paraconductivity measured in our work with the measurements of Suzuki and Hikita,[4] taken in LSCO films grown on the same substrate as ours and with a thickness of ~ 350 nm. We also take advantage of three important aspects with respect to most of the previous works: first, the high controllability of the doping level in the LSCO family has allowed us to grow c-axis oriented films with resistivities and transition widths among the best reported until now in this system.[1,4,23,24,26] Second, since the early results of Veira and Vidal[28] and Ramallo *et al.*,[29] it has been well-established experimentally that the MT contributions to $\Delta\sigma_{ab}$ are negligible in optimally doped HTSC. This also coincides with the calculations in Refs. 30,31 that indicate that for superconducting pairings with a d-wave component, the strong pair-breaking effects of impurities make the MT terms negligible. Experiments have also demonstrated the absence in the in-plane paraconductivity of optimally doped HTSC of the so-called density-of-states (DOS) contributions.[29] In our analysis of the underdoped and overdoped LSCO films, we will therefore assume the absence of appreciable indirect effects (MT and DOS). We will see how such an assumption is confirmed by the results of our experiments. A crucial advantage of our present work is to use recent extensions of the conventional mean-field-like calculations of $\Delta\sigma_{ab}$ to the short-wavelength regime $\varepsilon \gtrsim 0.1$.[32,33] These extensions are based on the introduction of a total-energy cutoff in the spectrum of the Gaussian-Ginzburg-Landau (GGL) superconducting fluctuations, which accounts for the Heisenberg localization energy associated with the shrinkage, when the reduced-temperature increases, of the superconducting wave function.[34] These ''extended'' GGL expressions have already allowed us to analyze the high-ε in-plane paraconductivity of the optimally doped YBCO,[32] and more recently the optimally-doped $Bi_2Sr_2CaCu_2O_{8+x}$ and $Tl_2Ba_2Ca_2Cu_3O_{10}$.[33] The high-ε paraconductivity in a single underdoped LSCO film, with $x \simeq 0.10$, was also briefly analyzed in Ref. 33. Note, however, that in that work, the superconducting fluctuations were assumed to be essentially 2D. As we will see in the present work, this is not the most likely

TABLE I. Summary of the main parameters of the LSCO thin films studied in this work. The T_{cI}, T_{cI}^-, and T_{cI}^+ temperatures are represented in Fig. 3. The $\xi_c(0)$ and ε^c main values are the ones resulting from the $\Delta\sigma_{ab}(\varepsilon)$ fits presented in Fig. 5. Their uncertainties result from considering different normal-state backgrounds (see Fig. 10 and main text).

x	Thickness (nm)	ρ_{ab}(250 K) ($\mu\Omega$ cm)	T_{cI} ($T_{cI}^- - T_{cI}^+$) (K)	$\xi_c(0)$ (Å)	ε^c
0.10	130	1200	21.1 (20.3–22.3)	0.9 (0.7–1.2)	0.8 (0.4–1.1)
0.12	150	830	23.8 (22.6–25.5)	0.8 (0.7–1.2)	0.7 (0.4–1.0)
0.15	150	580	27.2 (26.2–28.3)	0.9 (0.7–1.2)	0.8 (0.4–1.1)
0.20	150	310	26.3 (25.1–27.7)	0.5 (∼0–0.9)	0.8 (0.4–1.1)
0.25	120	230	14.8 (14.0–15.9)	∼0 (∼0–0.5)	0.7 (0.4–0.9)

scenario for our underdoped LSCO films in the $\varepsilon \lesssim 0.1$ region. In analyzing our data, we will clearly emphasize which results are expected to be independent of the structural nature of the samples and which concern the ''fine'' behavior of the paraconductivity and are therefore applicable only to thin films.

In Sec. II, we describe the samples' preparation and the resistivity measurements. The extraction from these data of the in-plane paraconductivity, and their analysis in terms of the GGL model for superconducting fluctuations with a total-energy cutoff, is presented in Sec. III. We summarize our conclusions and discuss their main implications in Sec. IV.

II. SAMPLES' PREPARATION AND ELECTRICAL RESISTIVITY MEASUREMENTS

The samples studied in this work are *c*-axis-oriented LSCO thin films grown on (100)$SrTiO_3$ substrates from ceramic single targets with different Sr contents. All the films have similar thickness, of around 150 nm (see Table I). During deposition, by high-pressure DC sputtering with an on-axis cathode-substrate configuration, the substrate was maintained at temperatures between 840 and 860 °C in a flow of pure oxygen at 1.3 Torr. After deposition, the films were kept for 30 min at the same temperature but at an oxygen pressure of 7–10 Torr. They were subsequently cooled to room temperature to ensure full oxygenation. The crystal structure of the LSCO films was studied by x-ray diffraction in a Bragg-Brentano geometry. The diffraction spectra exhibit only (00*l*) peaks, indicating an oriented growth with the *c* axis perpendicular to the substrate. The full width at half maximum of the rocking curve corresponding to the (006) reflection is around 0.3° for all the studied samples. Films were then patterned as narrow strips, with typical widths from 5 to 10 μm and typical lengths of 100 μm, by photolithography and wet chemical etching. Au contact pads were then deposited onto the current and voltage terminals, and annealed in oxygen at 1 atm and 600 °C for 15 min to facilitate gold diffusion into the LSCO. The final resistance achieved was less than 0.1 Ω per contact. The in-plane resistivity of the films, $\rho_{ab}(T)$, was then measured by using a standard four-contact DC current arrangement in a temperature range of 4.2–300 K. The applied current was ~ 5 μA, which implies that the current density through the sample is around 100 A cm^{-2} (much lower than the critical current density with no applied magnetic field). The resolutions in the $\rho_{ab}(T)$ measurement are about 1 $\mu\Omega$ cm for resistivity, and about 10 mK for temperature.

Figures 1–3 show the temperature dependence of $\rho_{ab}(T)$ for our LSCO thin films, with Sr contents of $x=0.10$, 0.12, 0.15, 0.20, and 0.25. These x values are those given by the nominal deposition rates. As the figures show, by increasing the Sr content, the in-plane resistivity gradually decreases and its T dependence well above T_c changes systematically from a concave shape (for $x \leqslant 0.15$) to a more linear one (for $x > 0.15$). Such a doping dependence of the resistivity is in good agreement with previous results in similar LSCO films.[1,4,23,24,26,33] The values of ρ_{ab} at 250 K in all the films studied here (see Table I) are among the lowest reported until now in the literature regarding LSCO films having the same doping and substrate and a similar thickness.[1,4,23,24,26,33] Another indication of the quality of our samples is the width of the superconducting transition in the $\rho_{ab}(T)$ curves, which are also among the smallest reported in the literature. Figure 3 shows the detail of $\rho_{ab}(T)$ around the superconducting transition and the corresponding $d\rho_{ab}/dT$, as well as T_{cI}, the temperature where $d\rho_{ab}/dT$ reaches its maximum, and T_{cI}^- and T_{cI}^+, which correspond to the half maximum of that derivative peak above and below T_{cI}, respectively. The values of T_{cI}, T_{cI}^-, and T_{cI}^+ for all the samples studied in this work are given in Table I. Also, in Fig. 4, we show the T_{cI} values of our films as a function of the Sr content. As the figure clearly shows, T_{cI} rises when the Sr content is increased up to an optimal doping level of about $x=0.15$, and then falls. These T_{cI} values, and their doping dependence, are in good agreement with those currently well established for T_c in LSCO films with similar substrate and thickness (note that the T_{cI} values of good-quality bulk LSCO are higher than in thin films with a similar Sr content, although both types of samples share the same T_{cI} dependence on doping).[1,4,23,24,26,33] In the remaining work we will use, unless specified otherwise, T_{cI} as T_c. The appropriateness of such a choice in the analysis of the in-plane paraconductivity will be discussed in further detail in Sec. III D.

III. THE IN-PLANE PARACONDUCTIVITY: COMPARISON WITH THE EXTENDED GGL APPROACH

A. Extraction of the in-plane paraconductivity

The paraconductivity may be obtained from the measured $\rho_{ab}(T)$ curves by the application of Eq. (1). For that, as is

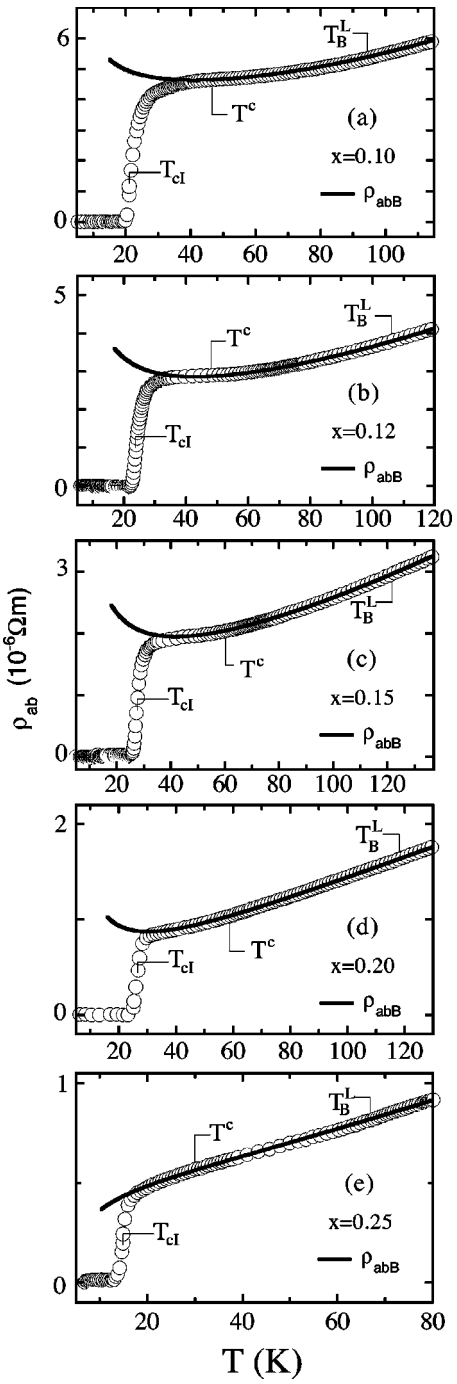

FIG. 1. The in-plane resistivity measured in this work (circles) in various LSCO thin films with different doping levels x. We also indicate (solid line) the normal-state background of each film, obtained by using the procedure indicated in the main text. The temperature T_B^L corresponds to the lower limit of the fitting region used to extract such background. The temperature T^c is the one at which the background and the experimental data first time deviate from each other (i.e., the temperature above which fluctuation effects are no longer observed). Note that T^c is located well below T_B^L (see also main text for details). T_{cI} is the temperature where $d\rho_{ab}/dT$ is maximum, which is expected to be close to T_c, the mean-field normal-superconductor transition temperature.

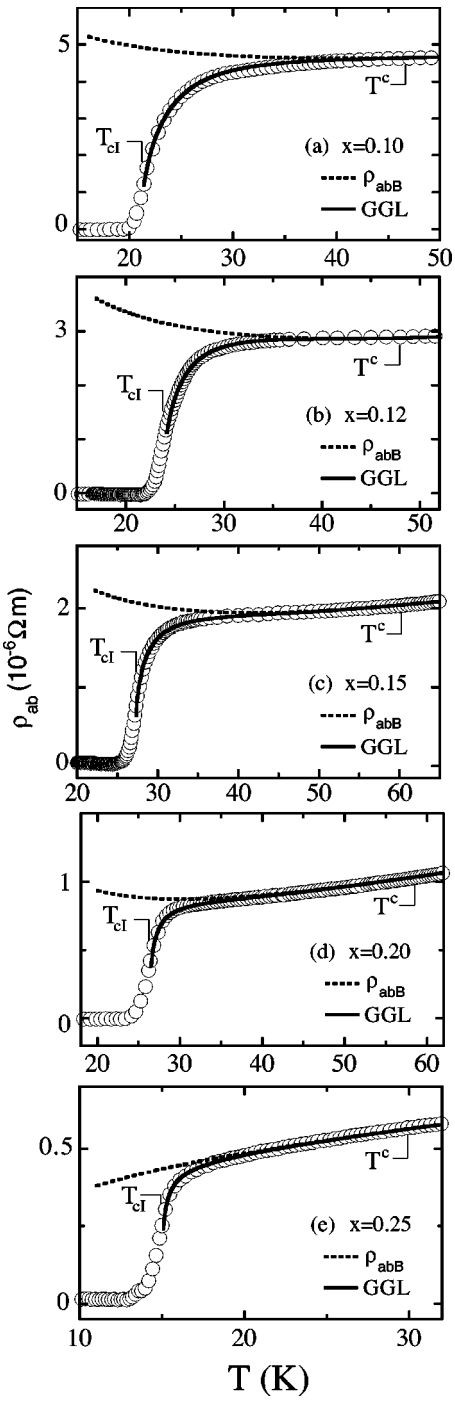

FIG. 2. Amplification of the view in Fig. 1 to appreciate better the range of temperatures where the fluctuation effects above the transition are observed. The dashed line corresponds to the normal-state background and the solid line corresponds to the theoretical $\rho_{ab}(T)$ obtained by using in Eq. (1) this background and the best fit by the GGL theory extended to high reduced temperatures through its regularization with the so-called ''total-energy'' cutoff which takes into account the quantum localization energy.

customary,[2,3] the normal-state background ρ_{abB} $(=\sigma_{abB}^{-1})$ is estimated by extrapolation of the $\rho_{ab}(T)$ data measured well above the ε-region where $\Delta\sigma_{ab}(\varepsilon)$ is to be analyzed. As we wish to analyze $\Delta\sigma_{ab}(\varepsilon)$ also in the high-ε ($\varepsilon > 0.1$) region,

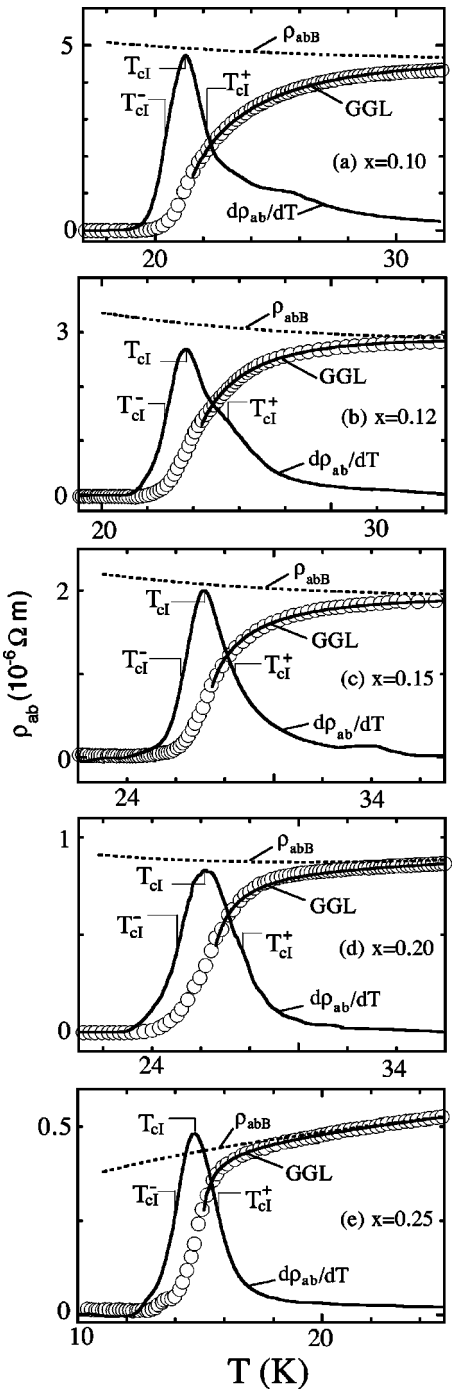

FIG. 3. Scoop of Figs. 1 and 2 to appreciate better the region closer to T_{cI}, the temperature where $d\rho_{ab}/dT$ is maximum. Such a $d\rho_{ab}/dT$ peak is also plotted, in arbitrary units (as a solid line). The temperatures T_{cI}^{-} and T_{cI}^{+} correspond to the half maximum boundaries of such a peak. The circles are the experimental $\rho_{ab}(T)$ data, the dashed line is the normal-state background, and the solid line following the data is the $\rho_{ab}(T)$ resulting from this background and the "extended" GGL theory with a total-energy cutoff.

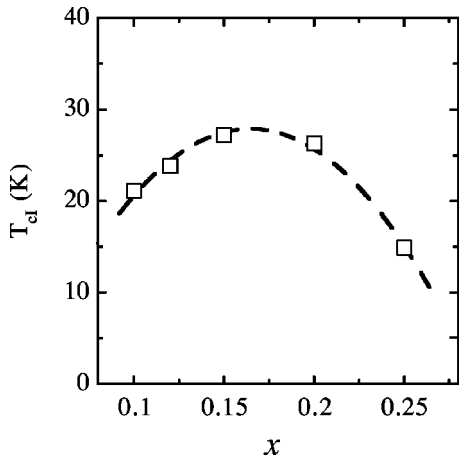

FIG. 4. The temperature T_{cI} where the inflexion point of the $\rho_{ab}(T)$ transition (see Figs. 2 and 3) is located versus the Sr content x in the LSCO films measured in this work. The dashed line is a parabolic fit which serves as a guide for the eyes. Note that both the absolute values and the doping dependence of such T_{cI} are in fairly good agreement with the ones well established[1,4,23,24,26,33] for the critical temperature of LSCO films grown on (100)$SrTiO_3$ substrates and with a similar thickness.

for such an extrapolation we will use a procedure similar to the one already used in Refs. 32,33. This is a two-step process to be done for each sample. First, we fit the functionality $a_1/T+a_2+a_3T$, with a_1, a_2, and a_3 as fitting parameters, to the $\rho_{ab}(T)$ data in the T region $1.6T_c \lesssim T \lesssim 2.7T_c$ (corresponding to $0.5 \lesssim \varepsilon \lesssim 1$). This is the simplest functionality which for all dopings gives a good coincidence with the $\rho_{ab}(T)$ data in that T range. Naturally, the background thus obtained is appropriate to analyze $\Delta\sigma_{ab}(\varepsilon)$ only for ε values well below $\varepsilon \simeq 0.5$. And, in fact, similar types of extrapolations have been successfully used to obtain $\Delta\sigma_{ab}(\varepsilon)$ up to $\varepsilon \simeq 0.1$ in various optimally doped HTSC (see, e.g., Refs. 3,28,29,35). However, by construction, this background makes $\Delta\sigma_{ab}$ zero at $\varepsilon = 0.5$, and thus cannot lead to a reliable study of $\Delta\sigma_{ab}(\varepsilon)$ in the high-ε ($\varepsilon > 0.1$) region. Therefore, the second step to be taken in determining a background valid for our purposes is to perform a fit to the $\rho_{ab}(T)$ data at considerably higher reduced temperatures, in the T range $4.5T_c \lesssim T \lesssim 7T_c$ (which corresponds to $1.5 \lesssim \varepsilon \lesssim 2$). However, because the extrapolation uncertainties strongly increase with increasing T distance, we constrain this last fit to reproduce in the moderate-ε range $10^{-2} \lesssim \varepsilon \lesssim 0.1$ the $\Delta\sigma_{ab}(\varepsilon)$ results obtained with our first background estimate, up to a $\pm 20\%$ maximum uncertainty. We also require that $\rho_{abB}(T)$ does not produce a negative paraconductivity at any temperature. We used for this fit the functionality $a_1/T+a_2+a_3T+a_4T^2$, with a_1, a_2, a_3, and a_4 as fitting parameters. This is the simplest functionality which for all dopings is able to fit the $\rho_{ab}(T)$ data in the enlarged fitting T region while at the same time fulfilling the abovementioned constrains.

In Figs. 1–3, we plot the normal-state backgrounds obtained by using the above procedure in all the films studied in this work. Note that the upwards concavity of $\rho_{abB}(T)$ diminishes for $x \geqslant 0.15$. For the $x = 0.25$ sample, our extrapolation method produces a $\rho_{abB}(T)$ curve with an appreciable negative curvature below T_c. However, in the T range of interest for our purposes (i.e., from T_c up to the upper limit

of the background fitting region, a range that in this film corresponds to 14.8 K$\lesssim T \lesssim$104 K), this $\rho_{ab}(T)$ may be approximated by the linear formula $\rho_{abB}(T)=(3.4\times10^{-7}\ \Omega\mathrm{m})+(7.2\times10^{-9}\ \Omega\mathrm{m\,K^{-1}})T$, the differences being less than 5%. Also shown in Figs. 1 and 2 is T^c, the temperature at which $\Delta\sigma_{ab}(\varepsilon)$ is observed to become negligible. Let us emphasize here that T^c is well below T_B^L, indicating therefore that the existence of such a T^c is not an artifact of our background subtraction procedure. This is further confirmed by the fact that the obtained backgrounds and corresponding T^c values do not appreciably depend on the lower limit of the background fitting region, T_B^L, provided that it is kept above $\sim 3.5T_c$ (i.e., above $\varepsilon \simeq 1.2$). An in-depth analysis of the uncertainties associated with our background estimation, including those associated with the choice of the background fitting region and its possible influence on T^c, will be presented later in Sec. III D.

In Fig. 5, we show the $\Delta\sigma_{ab}$-versus-ε curves obtained for each of the films measured in this work. This figure already illustrates a result which is central in our present paper: the experimental $\Delta\sigma_{ab}(\varepsilon)$ curves agree with each other well within the experimental errors for the doping levels $0.10 \leqslant x \leqslant 0.15$ (corresponding to the underdoped and optimally doped ranges of compositions). Note that this conclusion does not rely on any comparison with any theory. This striking result already suggests the nonvalidity, at least for LSCO films, of the proposals made by various authors (see, e.g., Refs. 1,12,14–17) that the superconducting fluctuations are substantially different in underdoped and optimally doped HTSC. As also shown in Fig. 5, in the overdoped range of compositions (i.e., for $x=0.20$ and 0.25), the in-plane paraconductivity of the LSCO films increases with the increasing value of x, mainly in the ε region $\varepsilon \lesssim 0.1$. At higher reduced temperatures, all the $\Delta\sigma_{ab}(\varepsilon)$ curves (for all x) collapse towards negligible paraconductivity at a reduced temperature ε of around 0.8.

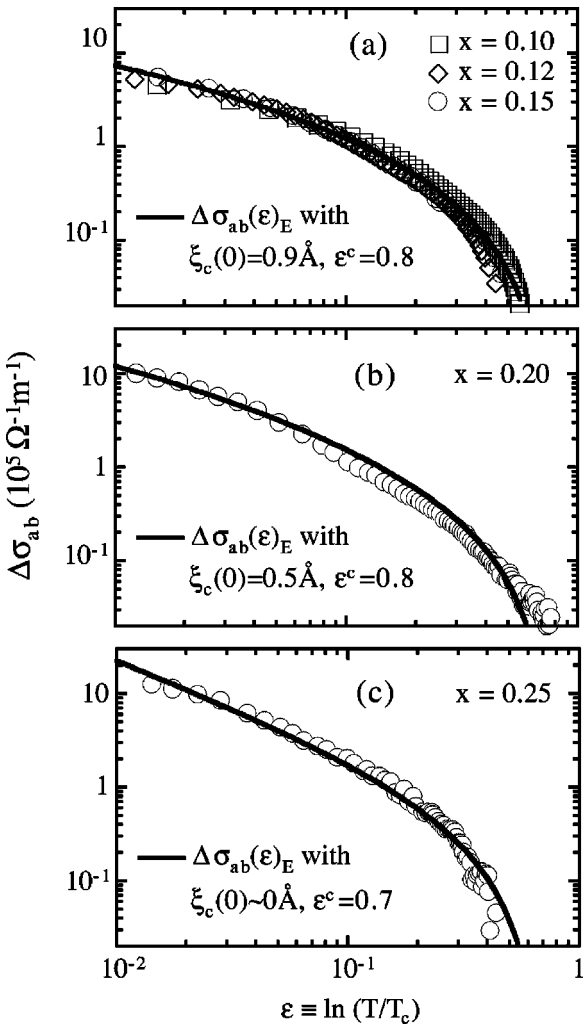

FIG. 5. Comparison between the "extended" GGL expressions for $\Delta\sigma_{ab}(\varepsilon)$ using a total-energy cutoff [solid lines, Eq. (8)] and the experimental curves of the in-plane paraconductivity versus reduced temperature in the LSCO films measured in this work (circles). In these comparisons, we use T_{cI} as critical temperature (see main text). As can be seen in (a), the experimental $\Delta\sigma_{ab}(\varepsilon)$ curves for the underdoped and optimally doped LSCO films are essentially coincident. The corresponding $\Delta\sigma_{ab}(\varepsilon)$ for the overdoped films [(b) and (c)] show a moderate increase as x increases. The GGL fits are able to account for such data in all the studied ε range, including also the disappearance of observable fluctuation effects at high reduced temperatures. See main text for details.

B. Theoretical background: extension of the GGL paraconductivity to the high-ε region

To analyze the experimental data summarized in the preceding section, we will use the paraconductivity expressions obtained on the grounds of the mean-field GGL approach regularized through the so-called "total-energy" cutoff, which takes into account the limits imposed by the uncertainty principle on the shrinkage of the superconducting wave function when the temperature increases well above T_c.[34] Our results in optimally doped HTSC suggest that such a regularization extends the applicability of the mean-field-like GGL approach from the $\varepsilon_{\mathrm{LG}} \lesssim \varepsilon \lesssim 0.1$ region to the high-ε region.[32–34] Here $\varepsilon_{\mathrm{LG}}$ is the so-called Levanyuk-Ginzburg reduced temperature, below which the fluctuations enter in the full-critical, non-Gaussian region where non-mean-field approaches (such as the 3DXY model) must be applied.[36] Such an $\varepsilon_{\mathrm{LG}}$ was estimated to be of the order of 10^{-2} in HTSC.[3,36] Note also that so close to T_c the effects of sample inhomogeneities may considerably affect the paraconductivity data.[27] Therefore, in the present paper, we will restrict our analyses to the mean-field-like $\varepsilon \gtrsim 10^{-2}$ region. Although the GGL in-plane paraconductivity under the total-energy cutoff was calculated for the first time by Carballeira *et al.* in Ref. 32, it will be useful to summarize in this section some of the results of such calculations for the case of single-layered superconductors, and also to remember the physical meaning of the total-energy cutoff, which was analyzed in terms of the uncertainty principle applied to the superconducting wave function by Vidal *et al.* in Ref. 34. For layered superconductors with a single interlayer separation s (the case of the LSCO family, where $s=6.6$ Å), the total-energy cutoff may be written as

$$k_{xy}^2+\frac{B_{\rm LD}[1-\cos(k_z s)]}{2\xi_{ab}^2(0)}+\xi_{ab}^{-2}(\varepsilon)\leqslant\xi_{ab0}^{-2}. \qquad (2)$$

In this expression, $\mathbf{k}_{xy}$ and $\mathbf{k}_z$ are the in-plane and *c*-direction wave vectors of the fluctuating modes, $\xi_{ab}(\varepsilon)=\xi_{ab}(0)\varepsilon^{-1/2}$ is the in-plane GL coherence length, $B_{\rm LD}\equiv[2\xi_c(0)/s]^2$ is the so-called Lawrence-Doniach (LD) dimensional crossover parameter, $\xi_{ab}(0)$ and $\xi_c(0)$ are, respectively, the in-plane and out-of-plane GL superconducting coherence length amplitudes, and ξ_{ab0} is the in-plane Pippard coherence length. Note that $\mathbf{k}_z$ is limited by the layered structure as $-\pi/s\leqslant k_z\leqslant\pi/s$.

The left-hand side of Eq. (2) is the total energy of a fluctuating mode (in units of $\hbar^2/2m_{ab}^*$, where $\hbar$ is the reduced Planck constant and m_{ab}^* is the in-plane effective mass of the superconducting pairs). As explained by Vidal *et al.* in Ref. 34, this ''total energy'' of each fluctuating mode may be seen as the sum of the Heisenberg localization energy associated with the shrinkage of the superconducting wave function when the temperature increases above T_c [the $\xi_{ab}^{-2}(\varepsilon)$ term] and the conventional kinetic energy. In the case of single-layered superconductors, the kinetic energy appears as the sum of the in-plane k_{xy}^2 and the *c*-direction $B_{\rm LD}[1-\cos(k_z s)]/2\xi_{ab}^2(0)$ contributions. The right-hand side of Eq. (2) may be seen as the localization energy associated with the maximum shrinkage, at $T=0$ K, of the superconducting wave function. This term is, therefore, proportional to the inverse square of the in-plane Pippard coherence length amplitude ξ_{ab0} (see Ref. 34).

To briefly analyze the differences between the total-energy cutoff and the conventional momentum or kinetic-energy cutoff, the simplest case is the 2D layered limit, where $B_{\rm LD}\to 0$. In that case, Eq. (2) simplifies to

$$k_{xy}^2+\xi_{ab}^{-2}(\varepsilon)\leqslant\xi_{ab0}^{-2}. \qquad (3)$$

Near T_c, when $\xi_{ab}(\varepsilon)\geqslant\xi_{ab0}$, the localization energy contribution to each fluctuating mode may be neglected and Eq. (3) reduces to the conventional momentum or kinetic-energy cutoff in 2D layered superconductors:[2]

$$k_{xy}^2\leqslant c\,\xi_{ab}^{-2}(0). \qquad (4)$$

In this equation, we have used $c^{-1/2}\xi_{ab}(0)$ instead of Pippard's ξ_{ab0}, where *c* is a cutoff amplitude, temperature independent, close to 1. These expressions still simplify in the case of isotropic 3D superconductors; the total-energy cutoff reduces to $k^2+\xi^{-2}(\varepsilon)\leqslant\xi_0^{-2}$, whereas one re-finds $k^2\leqslant c\,\xi^{-2}(0)$ for the momentum or kinetic-energy cutoff, which is the familiar condition earlier proposed for low-T_c superconductors.[2] By using $\xi_0=c^{-1/2}\xi(0)$ again and assuming the applicability at all reduced temperatures of the mean-field ε dependence of the superconducting coherence length, $\xi(\varepsilon)=\xi(0)\varepsilon^{-1/2}$, one may see that the conventional kinetic-energy and the total-energy cutoffs are related, in the 2D and 3D limits, through the substitution of *c* by $c-\varepsilon$. So, as stressed before, both cutoffs coincide near T_c, when $\varepsilon\ll c$. The conventional momentum or kinetic-energy cutoff appears, then, as a particular case, the limit when $\xi(\varepsilon)\gg\xi_0$, of the total-energy cutoff. However, in spite of this simple relationship between both cutoff approaches, first proposed by Mosqueira *et al.* in Ref. 37, their deep conceptual differences also lead to striking differences in the high-ε behavior of any observable associated with the superconducting fluctuations above T_c, including the paraconductivity. These differences have been analyzed in Refs. 32–34, but it might be useful to stress some of them here. First, note that the maximum in-plane kinetic energy of the fluctuating modes, $E_{ab,\rm kinetic}^{\rm max}$, is temperature independent in the case of the conventional kinetic-energy or momentum cutoff. For instance, for 2D layered superconductors,

$$E_{ab,\rm kinetic}^{\rm max}(\text{momentum cutoff})=\frac{(\hbar k_{xy}^{\rm max})^2}{2m_{ab}^*}=\frac{\hbar^2}{2m_{ab}^*\xi_{ab}^2(0)}c. \qquad (5)$$

In contrast, under a total-energy cutoff, the maximum in-plane kinetic energy of the fluctuating modes is temperature dependent. In this example (2D layered superconductors), the corresponding $E_{ab,\rm kinetic}^{\rm max}$ may be directly obtained from Eq. (5) by using $c-\varepsilon$ instead of *c* [or from Eq. (3) and using again $\xi_{ab0}=c^{-1/2}\xi_{ab}(0)$ and $\xi_{ab}(\varepsilon)=\xi_{ab}(0)\varepsilon^{-1/2}$] as

$$E_{ab,\rm kinetic}^{\rm max}(\text{total-energy cutoff})=\frac{\hbar^2}{2m_{ab}^*\xi_{ab}^2(0)}(c-\varepsilon),\quad \text{with } \varepsilon\leqslant c, \qquad (6)$$

which is temperature dependent and becomes zero for $\varepsilon\geqslant c$. In other words, in contrast with the conventional momentum or kinetic-energy cutoff which only eliminates, independent of the temperature, the fluctuating modes with in-plane kinetic energy above $c\hbar^2/2m_{ab}^*\xi_{ab}^2(0)$, the total-energy cutoff eliminates *all* the fluctuating modes at reduced temperatures equal to *c* or above. By imposing a zero kinetic energy on Eqs. (2) or (3), this reduced temperature, denoted ε^c, is given by

$$\xi_{ab}(\varepsilon^c)=\xi_{ab0}, \qquad (7)$$

i.e., $\varepsilon^c=(\xi_{ab}(0)/\xi_{abo})^2$. As first argued by Vidal *et al.* in Ref. 34, Eq. (6) (which leads directly to the existence of a well-defined reduced temperature above which all coherent Cooper pairs vanish) may be seen as just a consequence of the limitations imposed by the uncertainty principle on the shrinkage of the superconducting wave function, which also above T_c imposes the condition $\xi_{ab}(\varepsilon)\geqslant\xi_{ab0}$. In other words, the collective behavior of the Cooper pairs is dominated at high reduced temperatures by the Heisenberg localization energy.[34] If, in addition, we assume the applicability of the BCS relationship in the clean limit, $\xi_{ab}(0)=0.74\,\xi_{abo}$, then $\varepsilon_{\rm BCSclean}^c=c_{\rm BCSclean}\simeq 0.6$.[33,34,38] Indeed, this value of *c* will also apply to the conventional momentum cutoff approach that appears as the limit when $\varepsilon\ll 1$ of the total-energy cutoff.

As we are particularly interested in analyzing the dimensionality of the superconducting fluctuations in LSCO as a function of the doping, we will first summarize here the general expressions of the paraconductivity as a function of the

LD dimensional crossover parameter B_{LD}. Then we will also present the limiting cases $B_{\mathrm{LD}} \ll \varepsilon$ (2D limit) and $B_{\mathrm{LD}} \gg \varepsilon$ with $\xi_{ab}(0)=\xi_c(0)$ (isotropic 3D limit). The paraconductivity for single-layered superconductors, resulting from the GGL approach extended to high reduced temperatures by the total-energy cutoff, has been calculated by Carballeira *et al.* in Ref. 32 to be:

$$\Delta\sigma_{ab}(\varepsilon)_{\mathrm{E}}=\frac{e^2}{16\hbar s}\left[\frac{1}{\varepsilon}\left(1+\frac{B_{\mathrm{LD}}}{\varepsilon}\right)^{-1/2}-\frac{1}{\varepsilon^c}\left(2-\frac{\varepsilon+B_{\mathrm{LD}}/2}{\varepsilon^c}\right)\right], \tag{8}$$

where e is the electron charge. The paraconductivity under a total-energy cutoff in the 2D limit may then be obtained by applying in Eq. (8) condition $B_{\mathrm{LD}} \ll \varepsilon$:[32]

$$\Delta\sigma_{ab}^{2\mathrm{D}}(\varepsilon)_{\mathrm{E}}=\frac{e^2}{16\hbar s}\left[\frac{1}{\varepsilon}-\frac{1}{\varepsilon^c}\left(2-\frac{\varepsilon}{\varepsilon^c}\right)\right]. \tag{9}$$

Concerning the paraconductivity under a total-energy cutoff in the 3D limit, it cannot be directly obtained from Eq. (8) because this equation assumes the c-direction layered-structure cutoff, $-\pi/s \leqslant k_z \leqslant \pi/s$, which in the limit $B_{\mathrm{LD}} \gg \varepsilon$ is no longer a stronger limitation for k_z than the total-energy cutoff [Eq. (2)].[32] The calculations using the total-energy cutoff for the three directions of space have also been made in Ref. 32, the resulting expression for an isotropic superconductor being

$$\Delta\sigma_{ab}^{3\mathrm{D}}(\varepsilon)_{\mathrm{E}}=\frac{e^2}{48\pi\hbar\xi(0)}\left\{3\left[\frac{\arctan\left(\sqrt{(\varepsilon^c-\varepsilon)/\varepsilon}\right)}{\sqrt{\varepsilon}}-\frac{\varepsilon\sqrt{\varepsilon^c-\varepsilon}}{(\varepsilon^c)^2}\right]-5\frac{(\varepsilon^c-\varepsilon)^{3/2}}{(\varepsilon^c)^2}\right\}. \tag{10}$$

Let us also summarize the results for the in-plane paraconductivity under the conventional momentum cutoff. As first explicitly derived by Asaka *et al.*[9] (see also Ref. 32 for a more detailed calculation), the corresponding expression for a single-layered superconductor is

$$\Delta\sigma_{ab}(\varepsilon)_{\mathrm{M}}=\frac{e^2}{16\hbar s}\left\{\frac{1}{\varepsilon}\left(1+\frac{B_{\mathrm{LD}}}{\varepsilon}\right)^{-1/2}-\frac{c(c+\varepsilon+B_{\mathrm{LD}}/2)}{[(c+\varepsilon+B_{\mathrm{LD}})(c+\varepsilon)]^{3/2}}-\frac{1}{\varepsilon+c}\left(1+\frac{B_{\mathrm{LD}}}{\varepsilon+c}\right)^{-1/2}\right\}. \tag{11}$$

The corresponding results in the 2D and isotropic 3D limits are, respectively,

$$\Delta\sigma_{ab}^{2D}(\varepsilon)_{\mathrm{M}}=\frac{e^2}{16\hbar s}\left[\frac{1}{\varepsilon}-\frac{c}{(c+\varepsilon)^2}-\frac{1}{\varepsilon+c}\right], \tag{12}$$

and

$$\Delta\sigma_{ab}^{3\mathrm{D}}(\varepsilon)_{\mathrm{M}}=\frac{e^2}{48\pi\hbar\xi(0)}\left\{3\left[\frac{\arctan\left(\sqrt{c/\varepsilon}\right)}{\sqrt{\varepsilon}}-\frac{\varepsilon\sqrt{c}}{(\varepsilon+c)^2}\right]-5\frac{c^{3/2}}{(\varepsilon+c)^2}\right\}. \tag{13}$$

Equations (12) and (13) correspond to the expressions first obtained for these 2D and 3D limits by Gauzzi and Pavuna in Ref. 35.

It is also useful to note here the differences between the asymptotic behavior of $\Delta\sigma_{ab}(\varepsilon)$ under the two different cutoff conditions. For instance, as it is well known,[32,35] in the 2D limit, the conventional momentum cutoff predicts that $\Delta\sigma_{ab}^{2\mathrm{D}}(\varepsilon)_{\mathrm{M}}$ smoothly decays as ε^{-3} when $\varepsilon \gg c$. In contrast, as stressed before, the paraconductivity under a total-energy cutoff presents a singularity when $\varepsilon=\varepsilon^c=c$. Such a behavior is not describable through a critical exponent in ε. However, when ε approaches c from below, such a singular behavior may be described in terms of a power law in $|\tilde{\varepsilon}|$, where $\tilde{\varepsilon} \equiv \varepsilon - c$. In the 2D limit, this asymptotic behavior is

$$\Delta\sigma_{ab}^{2\mathrm{D}}(\tilde{\varepsilon})_{\mathrm{E}}=\frac{\mathrm{e}^2}{16\hbar s c^3}|\tilde{\varepsilon}|^2, \quad \text{for } \tilde{\varepsilon}\to 0^-. \tag{14}$$

The in-plane paraconductivity without any cutoff may be directly obtained from the above $\Delta\sigma_{ab}(\varepsilon)$ expressions by simply imposing $\varepsilon \ll \varepsilon^c$ on Eqs. (8)–(10) [or $\varepsilon \ll c$ on Eqs. (11)–(13)]. This leads to the well-known LD expression for a single-layered superconductor:

$$\Delta\sigma_{ab}(\varepsilon)_{\text{no cutoff}}=\frac{e^2}{16\hbar s}\frac{1}{\varepsilon}\left(1+\frac{B_{\mathrm{LD}}}{\varepsilon}\right)^{-1/2}, \tag{15}$$

which recovers, in the limits $B_{\mathrm{LD}} \ll \varepsilon$ and $B_{\mathrm{LD}} \gg \varepsilon$ with $\xi_{ab}(0)=\xi_c(0)$, the also well-known results by Aslamazov and Larkin for the paraconductivity without any cutoff in 2D and isotropic 3D superconductors:

$$\Delta\sigma_{ab}^{2\mathrm{D}}(\varepsilon)_{\text{no cutoff}}=\frac{e^2}{16\hbar s\varepsilon}, \tag{16}$$

and

$$\Delta\sigma_{ab}^{3\mathrm{D}}(\varepsilon)_{\text{no cutoff}}=\frac{e^2}{32\hbar\xi_c(0)}\varepsilon^{-1/2}. \tag{17}$$

Finally, let us stress here that all the above expressions for the in-plane paraconductivity [Eqs. (8)–(17)] implicitly assume a relaxation time for the superconducting fluctuations equal to the one given by the standard BCS mean-field approach, $\tau_0=(\pi\hbar/8k_{\mathrm{B}}T_c)\varepsilon^{-1}$.[39] They also consider that all indirect contributions (as the Maki-Thompson and the density-of-states ones) to $\Delta\sigma_{ab}(\varepsilon)$ are negligible, as is today well established for the HTSC.[28,29]

C. Comparison between the experimental data and the GGL paraconductivity

In Fig. 5, we present a comparison between the theoretical predictions under a total-energy cutoff and the experimental

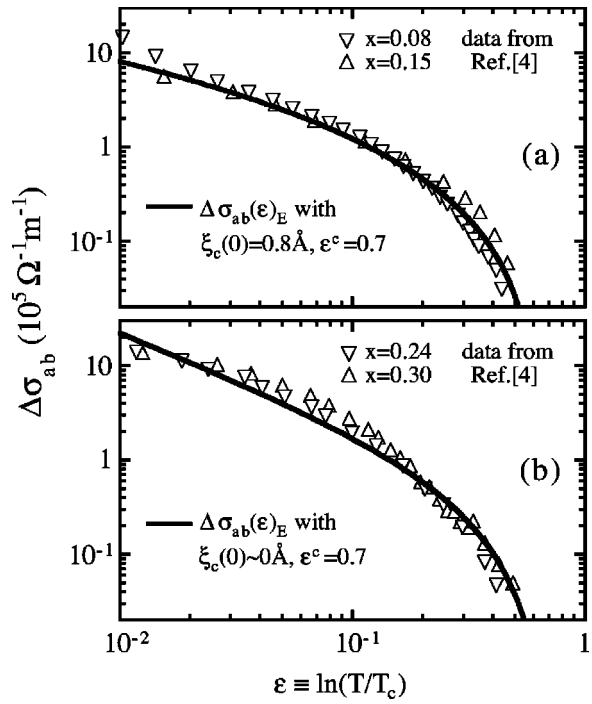

FIG. 6. Some examples of the in-plane paraconductivity versus reduced temperature curves that result from applying the same analyses as we have applied to our present measurements to the $\rho_{ab}(T)$ data measured by Suzuki and Hikita[4] in LSCO films. The solid lines correspond to the fits using the "extended" GGL approach with a total-energy cutoff. Such fits fully confirm the results found with our own measurements (compare, e.g., with Fig. 5).

paraconductivity obtained by using the procedure described in Sec. III A in our LSCO films. The solid lines in these figures are the best fits of Eq. (8) to the experimental paraconductivity in the ε-region ranging from 10^{-2} up to the reduced-temperatures where the paraconductivity becomes experimentally unappreciable (i.e., roughly when $\Delta\sigma_{ab} \simeq 2 \times 10^3\ \Omega^{-1}\,m^{-1}$). In these fits, we leave $\xi_c(0)$ and ε^c as free parameters, and use for T_c the inflexion point temperature at the $\rho_{ab}(T)$ transition, T_{cI}. The values thus obtained for $\xi_c(0)$ and ε^c are summarized in Table I. The errorbars and the x dependence of these values will be discussed later in detail. As is easily observable in this Fig. 5, for all the samples, the agreement between Eq. (8) and the experimental data is excellent in the entire studied ε region. This comparison confirms, in particular, the existence of a well-defined reduced temperature, ε^c, of about $\varepsilon^c \sim 0.8$, above which the in-plane paraconductivity vanishes. A different view of these fits is provided by Figs. 2 and 3. In these figures, the continuous lines are the theoretical $\rho_{ab}(T)$ curves which result from the above analyses [i.e., from adding, through Eq. (1), the normal-state background and the theoretical $\Delta\sigma_{ab}(\varepsilon)$ resulting from the above fits]. As visible in these figures, the agreement with the $\rho_{ab}(T)$ measurements above the transition is again excellent.

It may be useful to check if the GGL theory with a total-energy cutoff may also explain the in-plane resistivity measurements done by Suzuki and Hikita[4] in their own LSCO films, with various x values, grown on the same substrate as ours, and with a thickness of ~350 nm. For that, we have scanned the corresponding published $\rho_{ab}(T)$ plots[4] and have applied to these data the same analysis as described above. Some examples of the $\Delta\sigma_{ab}(\varepsilon)$ curves thus obtained, and their comparison with Eq. (8), are shown in Fig. 6. As it is evident in this figure, the GGL approach with a total-energy cutoff also explains these measurements, again in the $10^{-2} \lesssim \varepsilon \lesssim 1$ range. These data also confirm the existence of a well-defined reduced temperature, ε^c, above which the in-plane paraconductivity vanishes. We emphasize that in performing these analyses, we have again used T_{cI} as T_c and have not included any Maki-Thompson (MT) indirect contribution to the in-plane paraconductivity (which, as commented in the Introduction, are now well established to be absent in the HTSC[28,29]). As noted before, Suzuki and Hikita assumed in their analyses the existence of such MT contribution. In fact, to be able to introduce the MT contribution, Suzuki and Hikita had to consider the critical temperature as an additional adjustable parameter. This led to T_c appreciably different from T_{cI}. Our present analysis of Suzuki and Hikita's data also indicates that the in-plane paraconductivity in LSCO films grown in (100)$SrTiO_3$ substrates is, as could be expected, almost independent of the thickness in the range 150–350 nm. However, let us stress again that using bulk samples, or films grown on different substrates or with significantly different thickness, may change some of the fine details of the paraconductivity, such as the corresponding $\xi_c(0)$ values (see also below).

In Fig. 7, we show the comparison between the experimental $\Delta\sigma_{ab}(\varepsilon)$ measured in the present work and the paraconductivity expressions without any cutoff and under the conventional momentum or kinetic-energy cutoff, using the same values for $\xi_c(0)$ and ε^c as in Fig. 5. This figure shows that, as could be expected, the momentum or kinetic-energy cutoff expressions are able to fit the experimental paraconductivity in a lower ε range than the total-energy cutoff (up to $\varepsilon \simeq 0.3$ at the most for the momentum cutoff, and up to about $\varepsilon \simeq 0.1$ for no cutoff). In particular, they fail to reproduce the rapid fall off of the fluctuations in the higher-ε region, $\varepsilon \gtrsim 0.3$.

Let us now discuss the doping dependence of the parameters $\xi_c(0)$ and ε^c which results from the above fits using the GGL approach under a total-energy cutoff. In Fig. 8 we show these $\xi_c(0)$ and ε^c values as a function of the doping. Let us first remark on the trend for the variation of $\xi_c(0)$ with the doping level x; for $x \leqslant 0.15$, i.e., in the underdoped and optimally doped ranges, $\xi_c(0)$ is found to be approximately equal to 0.9 Å. This value corresponds to a LD dimensional crossover parameter $B_{\rm LD} \simeq 7.5 \times 10^{-2}$. For $x = 0.20$, it is $\xi_c(0) \simeq 0.5$ Å (and hence $B_{\rm LD} \simeq 2 \times 10^{-2}$), and for $x \simeq 0.25$ and above, it is $\xi_c(0) \sim 0$ Å (so $B_{\rm LD} \sim 0$ and the fluctuations are 2D in all the studied ε range). This $\xi_c(0)$-versus-x trend is consistent with our observation that the fluctuation conductivity is the same for the underdoped and optimally doped LSCO films, and increases with increasing x in the overdoped ones. Let us also note that in Refs. 23–25, it has been argued that the substrate may induce in LSCO films c-direction stress, which in turn may change the interlayer

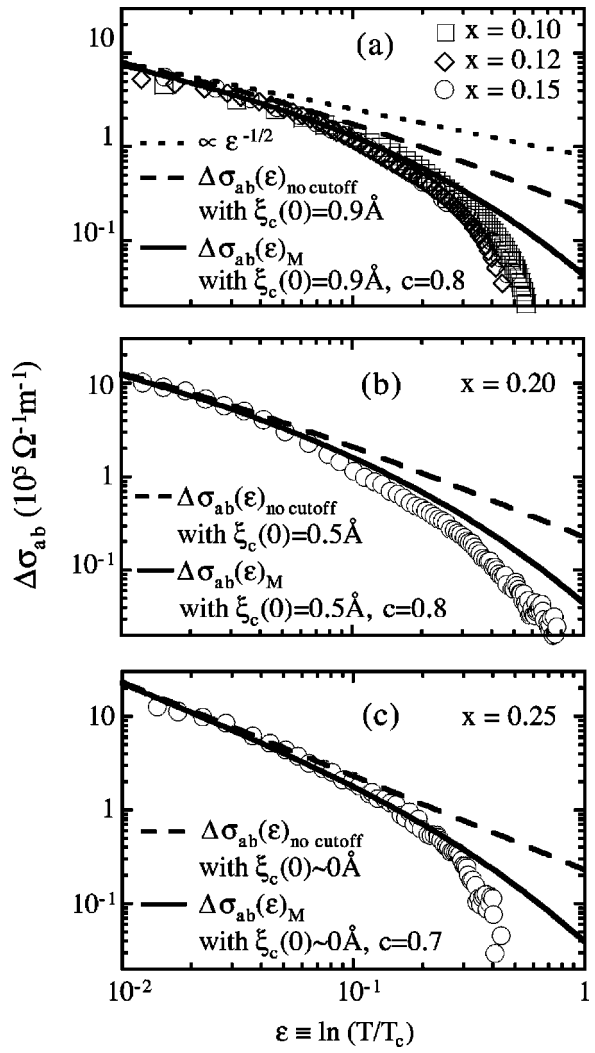

FIG. 7. Comparison between the same experimental curves as in Fig. 5 and the paraconductivity expressions without any cutoff [dashed lines, Eq. (15)] and with the momentum or kinetic-energy cutoff [continuous lines, Eq. (11)]. In performing these comparisons, we have used the same values for $\xi_c(0)$ and the cutoff constant as in Fig. 5. In (a), we also indicate the low-ε asymptotic $\Delta\sigma_{ab}(\varepsilon) \propto \varepsilon^{-1/2}$, which would correspond to the 3D limit without any cutoff. The dashed line in (c) also corresponds to $\Delta\sigma_{ab}(\varepsilon) \propto \varepsilon^{-1}$, i.e., the 2D limit without any cutoff. The $\varepsilon \sim 10^{-2}$ paraconductivity of the $x=0.20$ film does not follow any of these dimensionality limit cases, but lies instead in the dimensional crossover regime. Note that the momentum or kinetic-energy cutoff expressions are able to explain the experimental paraconductivity in a lower ε range than the total-energy cutoff (up to at most $\varepsilon \simeq 0.3$). The expressions without any cutoff explain the data in a even more limited ε range, $\varepsilon \lesssim 0.1$.

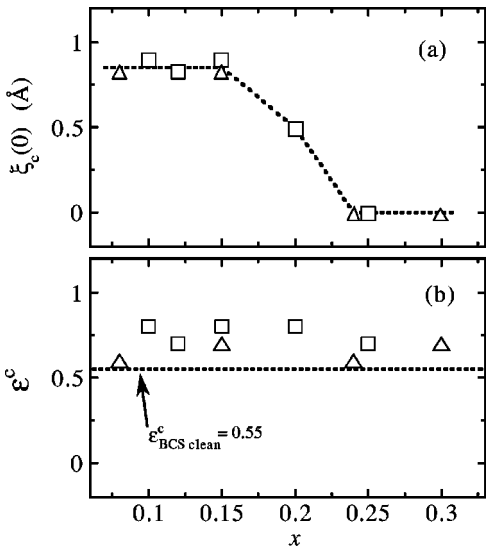

FIG. 8. The values of the *c*-direction coherence length GL amplitude $\xi_c(0)$ and of the total-energy cutoff amplitude ε^c, providing the best fit to the $\Delta\sigma_{ab}(\varepsilon)$ data (see Figs. 5 and 6), represented versus the Sr content (i.e., hole doping) x. The squares correspond to the LSCO films measured in the present work, while the triangles correspond to the films measured by Suzuki and Hikita[4] analyzed in Fig. 6. As can be easily seen in (a), $\xi_c(0)$ is constant, well within the experimental uncertainties, for the underdoped ($x<0.15$) and optimally doped ($x=0.15$) films. When entering in the overdoped range ($x>0.15$), $\xi_c(0)$ decreases to the point of being negligible [$\xi_c(0) \simeq 0$ Å] at about $x \simeq 0.25$ and above. The dashed line in (a) is guide for the eyes. (b) illustrates that the cutoff amplitude ε^c is found to be, within the experimental uncertainties, constant for all doping levels. The continuous line in (b) is the rough estimate $\varepsilon^c_{\mathrm{BCSclean}} \simeq 0.6$ which can be obtained by using the BCS theory in the clean limit (see main text). Note that the ε^c values shown in this figure are somewhat above this estimate. However, such differences cannot be taken as significative, in view of the errorbars of ε^c in our $\Delta\sigma_{ab}(\varepsilon)$ analyses (see main text and Table I).

tunneling. Therefore, LSCO films grown on different substrates or with significantly different film thickness, and also LSCO bulk samples, may have $\xi_c(0)$ values different to the ones found in the present work. In this sense, we have found, through measurements of the fluctuation-induced magnetization, that the superconducting fluctuations are bidimensional in underdoped *bulk* LSCO samples, in contrast with our present results for thin films.[40] It has also been found in Refs. 41,42 that the superconducting bidimensionality is smeared or suppressed in the overdoped bulk samples of the LSCO family. The comparison of these observations with our present results suggests, then, that the substrate effects in LSCO films do affect $\xi_c(0)$ and, therefore, the interlayer tunneling of Cooper pairs.

Concerning the other free parameter in our $\Delta\sigma_{ab}(\varepsilon)$ fits, ε^c, we find that its value remains the same within the experimental uncertainties for all the studied LSCO films (see Fig. 8 and Table I). Such a value which, taking into account its experimental uncertainty (mainly associated with the background subtraction, see below), is bound by $0.4 \lesssim \varepsilon^c \lesssim 1.1$ matches fairly well the value ~ 0.6, which may be roughly estimated on the grounds of the mean-field ε dependence of $\xi_{ab}(\varepsilon)$ and the BCS value of $\xi_{ab}(0)/\xi_{abo}$ in the clean limit (see Sec. III B and Ref. 34). We note that the validity of such a simple estimate has also been confirmed, usually with a lower error bar, by the analysis of the superconducting fluctuations in various optimally doped HTSC and various clean and moderately dirty LTSC (see Ref. 34, and references therein). We note also that our previous analyses of the

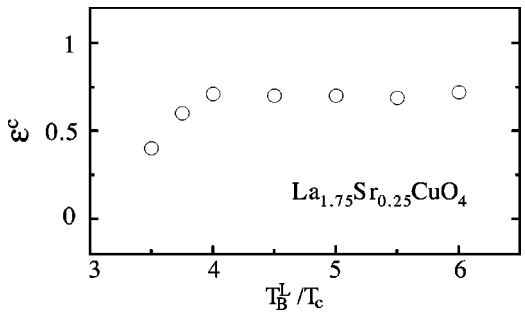

FIG. 9. An example, corresponding to the $x=0.25$ film, of the variation of ε^c with the temperature region where the background fit is made. T_B^L is the lower-temperature limit of this region. The upper limit was always taken to be T_B^L+40 K. Here again, we use T_{cI} as T_c. Note that the values obtained for ε^c are essentially independent of the region where the background fit is made unless T_B^L is relatively close to the transition. A similar conclusion is obtained for all the samples studied in this work.

fluctuation magnetization in a bulk underdoped LSCO led to $\varepsilon^c \simeq 0.6 \pm 0.2$. This is consistent with the fact that, as already mentioned in Sec. III B and further elaborated in Ref. 34, the appearance of the reduced-temperature cutoff ε^c is expected to occur in all superconductors independent of, e.g., their structural character or the dimensionality of the superconducting fluctuations.

D. On the influence of the background and T_c choices

It is relevant to discuss in detail the main sources of uncertainties in the above analyses of the experimental paraconductivity in terms of the extended GGL approach. Let us first consider the uncertainties associated with the extraction of the normal-state background contribution, $\rho_{abB}(T)$. We have checked that varying the lower limit of the background fitting region from its value in our analyses, $T_B^L=4.5T_c$, does not significantly change the obtained $\Delta\sigma_{ab}(\varepsilon)$ curves, provided that T_B^L is kept well above $\sim 3.5T_c$. In Fig. 9, we plot the ε^c values obtained by applying the analysis described in the previous sections to the $x=0.25$ LSCO sample by using different values of T_B^L. When obtaining this figure we have always taken the upper limit of the background fitting region as T_B^L+40 K. As it may be seen in this Fig. 9, ε^c is quite insensitive to T_B^L unless the latter is approximately $3.5T_c$ or lower. This indicates that the criterion $T_B^L \simeq 4.5T_c$ is adequate for obtaining values of ε^c not affected by the proximity of the background fitting region. We have also checked that adding a third degree polynomial term to the background functionality does not appreciably change the obtained paraconductivity curves. Similarly, we have also checked that using a variable-range-hopping contribution, $\rho_1 \exp(T_0/T)^{1/4}$, instead of the a_1/T term (as proposed, e.g., by Leridon *et al.*[13] when analyzing the high-ε paraconductivity of YBCO films), does not change the obtained backgrounds, within a maximum of 2% variation. However, a much more appreciable source of uncertainty comes from the fact that in our two-step procedure for obtaining the normal-state background (see Sec. III A), we allow it to produce $\Delta\sigma_{ab}$ results

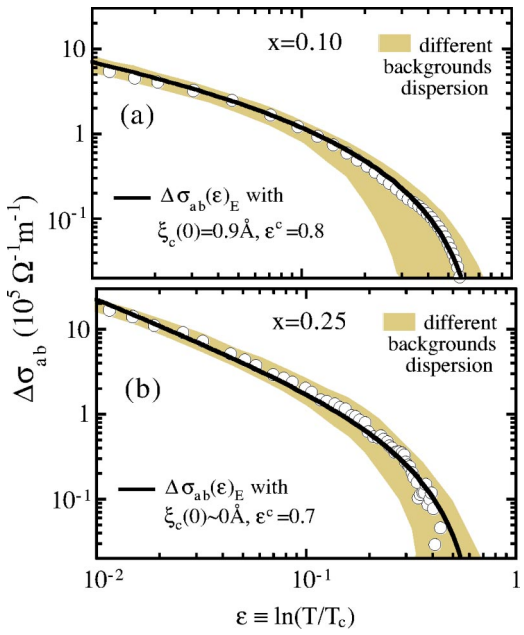

FIG. 10. Influence of the use of different normal-state backgrounds in the experimental $\Delta\sigma_{ab}(\varepsilon)$ curves of (a) the $x=0.10$ film and (b) the $x=0.25$ film measured in this work. The different sources of such a background uncertainty are discussed in detail in the main text. The corresponding uncertainties in ε^c and $\xi_c(0)$ are summarized in Table I for all the films measured in this work.

which deviate by $\pm 20\%$ at $10^{-2} \lesssim \varepsilon \lesssim 0.1$ from the $\Delta\sigma_{ab}$ results obtained with the background fitted closer to the transition (fitted in the T region $1.6\,T_c \lesssim T \lesssim 2.7\,T_c$, i.e., $0.5 \lesssim \varepsilon \lesssim 1$). The $\pm 20\%$ figure was chosen after verifying that it is a good measure of the variation of such "low-ε background" when its fitting region is somewhat varied. While this uncertainty has a relatively low impact on the $\Delta\sigma_{ab}(\varepsilon)$ curves for $10^{-2} \lesssim \varepsilon \lesssim 0.1$, its influence becomes stronger in the high reduced-temperature region ($\varepsilon > 0.1$), affecting mainly the precise value of ε^c (or, equivalently, of T^c). In particular, lower backgrounds indeed lead to lower ε^c and T^c. However, let us emphasize that this uncertainty does not affect the qualitative shape of the sharp fall off of $\Delta\sigma_{ab}$ at high reduced temperatures, but only the precise location of such a fall off. In Fig. 10, we illustrate the uncertainty of the $\Delta\sigma_{ab}(\varepsilon)$ curves associated with the choice of the background. The limits of the shaded areas correspond to the lower and higher backgrounds obtained for each sample. This figure clearly illustrates that the background uncertainty does not affect the low-ε region in a dramatic way, and therefore its impact on the value of $\xi_c(0)$ is also moderate. Table I summarizes the corresponding ε^c and $\xi_c(0)$ uncertainties for all the LSCO films measured in this work.

It may also be useful to study the influence of the T_c choice in our analyses. First of all, we note that the $d\rho_{ab}/dT$ peaks around T_{cI} present about 1 K of half widths at half maximum of the peak (see Fig. 3 and Table I). Taking into account the relatively low critical temperature of the LSCO family, such widths correspond to rather high reduced temperatures, of the order of $\varepsilon \sim 5 \times 10^{-2}$. This means that varying T_c inside the upper half of the T_{cI} peak may considerably

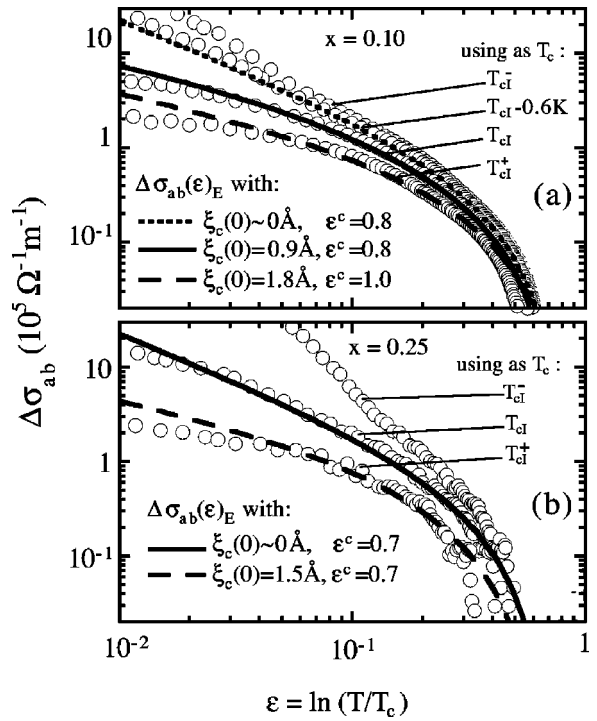

FIG. 11. Influence of the choice of T_c in the experimental $\Delta\sigma_{ab}(\varepsilon)$ curves and GGL fits, for (a) the $x=0.10$ film and (b) the $x=0.25$ film measured in this work. The T_c choice varies mainly the $\Delta\sigma_{ab}(\varepsilon)$ slope in the $\varepsilon\lesssim 0.1$ region. As is easily seen in these figures, using T_c below T_{cI} does not allow to fit the data with Eq. (8) for all the doping levels, and T_c above T_{cI} produces poorer fits than T_{cI}. The other underdoped and optimally doped films studied in this work produce curves similar to the $x=0.10$ ones, and the $x=0.20$ film produces results in between those of (a) and (b).

affect the paraconductivity versus reduced-temperature curves in a sizable ε region of our $\Delta\sigma_{ab}(\varepsilon)$ fits. Such uncertainty is illustrated in Fig. 11 for the cases $x=0.10$ and 0.25; in this figure, the same $\Delta\sigma_{ab}$ data as in Fig. 5 are plotted against $\varepsilon\equiv\ln(T/T_c)$ for T_c values in between T_{cI}^- and T_{cI}^+ (the lower and upper temperature boundaries of the T_{cI} peak at half maximum). Also plotted is Eq. (8) in those cases where it is possible to find $\xi_c(0)$ and ε^c values producing a valid agreement with such $\Delta\sigma_{ab}(\varepsilon)$ data curves. As is clearly illustrated by the figure, using T_c's below T_{cI} makes $\Delta\sigma_{ab}(\varepsilon)$ increase, and T_c's above T_{cI} makes $\Delta\sigma_{ab}(\varepsilon)$ decrease. In the case $x=0.10$, when lowering T_c, it is possible to fit Eq. (8) up to T_c values $T_c=T_{cI}-0.6$ K ($=T_{cI}^-+0.2$ K). This is accomplished by lowering $\xi_c(0)$, while the parameter ε^c remains almost unchanged from $\varepsilon^c=0.8$. In fact, using $T_c=T_{cI}-0.6$ K already leads to a fit with $\xi_c(0)\sim 0$ Å; because of this, with lower T_c's Eq. (8) can no longer account for the data. In the case of the $x=0.25$ film, $\xi_c(0)\sim 0$ Å already corresponds to $T_c=T_{cI}$ and hence the $\Delta\sigma_{ab}(\varepsilon)$ curves cannot be successfully fitted by Eq. (8) if using any T_c below T_{cI}. Let us now discuss what happens when using T_c's above T_{cI} instead of below. In this case, the $\Delta\sigma_{ab}(\varepsilon)$ curves decrease. Such a decrease can be reproduced to some extent by Eq. (8), for all the doping levels, by increasing $\xi_c(0)$ and slightly changing also ε^c. However, as shown in Fig. 11, the resulting fits are always of somewhat inferior quality than when using T_{cI}. To sum up, using T_{cI} as T_c seems to be the best choice because of the consistency when taking into account the data of films with different doping levels, and because it provides better-quality fits than T_c's taken above T_{cI}. However, we think that it is useful to bear in mind the conclusion that relatively small deviations from T_{cI} will have an appreciable impact on the values of $\xi_c(0)$. In particular, the $\xi_c(0)$ values obtained for each LSCO film using T_{cI}^+ instead of T_{cI} are 1.8 Å for $x=0.10$, 2.0 Å for $x=0.12$, 1.9 Å for $x=0.15$, 1.6 Å for $x=0.20$, and 1.5 Å for $x=0.25$. Also, for all the doping levels studied here, it is possible to find a T_c in between T_{cI}^- and T_{cI} leading to $\xi_c(0)\simeq 0$ Å. In fact, such uncertainties add to the reasons commented on in the Introduction that explain the discrepancies between different authors when proposing values for $\xi_c(0)$ from the analysis of the superconducting fluctuations in LSCO. For instance, in a previous work,[33] we briefly analyzed a single LSCO film, with $x=0.10$, assuming $\xi_c(0)\simeq 0$ Å, what led us to conclude that T_c was nearer to T_{cI}^- than to T_{cI}. Finally, let us emphasize here that in our present analyses, when using any choice of T_c with similar displacements with respect to T_{cI} for all the x values, our main qualitative conclusions remain true: the paraconductivity is constant with x in the underdoped and optimally doped LSCO thin films, but increases with x in the overdoped range up to $x\simeq 0.25$. Also, the choice of T_c does not affect the fact that the fluctuations sharply decrease at a well-defined reduced temperature well above T_c.

It may also be interesting to briefly discuss whether long-length-scale crystal imperfections (much bigger in size than the coherence length) may significantly affect our main experimental results. First of all, let us note that correcting for such extrinsic imperfections (for instance, by introducing a quality factor[43,44]) would always lead to higher intrinsic paraconductivity, as the imperfect samples would be less conductive than the ideal ones. Note also that such corrections may be expected to be essentially T independent, and therefore they would not significantly affect the critical exponents of the $\Delta\sigma_{ab}(\varepsilon)$ curves, but only their amplitudes. Comparison with the existing literature reveals that the resistivity at 250 K of our samples is never more than 1.2 times the one reported until now by different groups in LSCO films with the same doping and substrate and similar thickness (in fact, in several cases, our films are the less resistive ones).[1,4,23,24,26,33] Dividing the $\rho_{ab}(T)$ data by a quality factor of approximately 1.2 would not alter significantly our conclusions, as it would correspond to a $\sim$20% change in the amplitude of the $\Delta\sigma_{ab}(\varepsilon)$ curves, which is, in fact, lower than the uncertainty caused by other sources of ambiguity discussed above in this section.

IV. CONCLUDING REMARKS

In this paper, we have presented measurements of the in-plane paraconductivity $\Delta\sigma_{ab}$ above the superconducting transition of various high-quality LSCO thin films with a thickness of $\sim$150 nm grown on (100)$SrTiO_3$ substrates, with doping levels x varying from 0.10 to 0.25, in the re-

duced temperature range $10^{-2} \lesssim \varepsilon \lesssim 1$. Our results confirm, and extend to high reduced temperatures, the earlier proposals by Suzuki and Hikita[4] and by Cooper *et al.*[5] that in HTSC the variation of $\Delta\sigma_{ab}$ with doping may explain only a small part of the variation of the total in-plane conductivity σ_{ab} near T_c. In fact, for the underdoped and optimally doped compositions, our results directly show that the corresponding $\rho_{ab}(T)$ varies appreciably whereas the $\Delta\sigma_{ab}(\varepsilon)$ curves agree with each other well within the experimental uncertainties. Our results also show that in the overdoped regime, $\Delta\sigma_{ab}(\varepsilon)$ increases only moderately with increasing x. The absence of important anomalous doping effects on the paraconductivity is confirmed by the fact that our $\Delta\sigma_{ab}(\varepsilon)$ data may be appropriately accounted for by the GGL approach, extended to the high-ε region ($\varepsilon \gtrsim 0.1$) by means of a total-energy cutoff. The fits using such an approach lead to c-direction superconducting coherence length amplitudes $\xi_c(0)$ of about 0.9 Å for the underdoped and optimally doped films, about 0.5 Å for the $x=0.20$ overdoped film, and $\xi_c(0)$ negligibly small (~ 0 Å) for the $x=0.25$ one. Moreover, independent of the doping, we observe in all these LSCO films, a rapid decrease of the superconducting fluctuation effects in the high-ε region. Such a decrease is also well explained by the GGL approach with a total-energy cutoff, which, as shown by Vidal *et al.* in Ref. 34, takes into account the quantum localization energy associated with the limits imposed by the uncertainty principle on the shrinkage of the superconducting wave function as ε increases.

Concerning the fine behavior of the in-plane paraconductivity with doping, our results also confirm the proposal by Suzuki and Hikita[4] that in LSCO films the main effect of doping on the superconducting fluctuations is to change the c-direction superconducting coherence length $\xi_c(0)$. However, because of the use of MT terms in their analyses, these authors concluded that $\xi_c(0)$ would increase as x increases in the underdoped, optimally doped, and overdoped regimes. In contrast, we have shown here that when such terms are considered to be negligible, one obtains a different doping dependence of $\xi_c(0)$, as summarized above. As the absence of MT and DOS contributions to the in-plane paraconductivity is at present well established,[28,29] we believe that the true behavior of $\xi_c(0)$ with doping in LSCO thin films grown in $(100)SrTiO_3$ substrates is probably the one we propose here. Let us also note that the dependence of $\xi_c(0)$ with doping found here in LSCO films may be not applicable to LSCO bulk samples, as the substrate may also change $\xi_c(0)$ and, therefore, the dimensionality of the superconducting fluctuations. In particular, through measurements of the fluctuation-induced magnetization, it has been found[40] that the superconducting fluctuations are bidimensional in underdoped *bulk* LSCO samples, in contrast with our present results for thin films. In Refs. 41,42 it has also been found that the superconducting bidimensionality is smeared or suppressed in the overdoped bulk samples of the LSCO family. These differences between thin films and bulk samples of LSCO seem to be due in part to strain effects associated with the growth on a substrate with ab-plane lattice constants different to those of bulk LSCO.[22–25] Proposals that the main effect of doping on the superconducting fluctuations is to change $\xi_c(0)$ were also done (and almost simultaneously to Suzuki and Hikita[4]) for the YBCO compound by Cooper *et al.*[5] (and later by Juang *et al.*[8]). We note, however, that our present results cannot be directly extrapolated to YBCO because in this compound, doping occurs in the interlayer CuO chains, absent in LSCO. Such CuO chains are expected to determine most of the interlayer tunneling in YBCO due to their metallicklike character.

Another central result of our analyses is that the cutoff parameter ε^c arising in the ''extended'' GGL approach is found to be independent of the doping, well within the experimental uncertainties. As the conventional momentum cutoff is just a particular case, valid for $\varepsilon \lesssim 0.2$, of the total-energy cutoff approach, our conclusion will then apply to any analysis in terms of such a momentum cutoff. This suggests, therefore, that the doping dependence of the momentum cutoff observed in other HTSC compounds (see, e.g., Refs. 9 and 10) could be an extrinsic effect due to the presence of sample inhomogeneities or due to ambiguities in the background estimate.

Our results may also have implications on other open problems of the HTSC. First of all, they allow us to conclude, as mentioned in the title of this paper, that the superconducting fluctuations in underdoped LSCO films are not linked to the opening of their normal-state-pseudogap; first, because the changes of doping in such underdoped compounds, which are known to vary the pseudogap opening temperature T^*,[1] do not result in any observable change of the superconducting fluctuations, even in the high-ε region and second, because in such underdoped compositions, the superconducting fluctuations have also been found to disappear at reduced temperatures which are, even when taking into account the experimental uncertainties, always below 1.1, i.e., much below T^* (that is located above room temperature for the underdoped compositions studied in this work[1]). In other words, our experimental results seem to be contradictory with the theoretical proposals that in HTSC the superconducting fluctuations are strongly enhanced by underdoping.[1,12,14–17] Such proposals include, e.g., the ones where the pseudogap effects observed in the underdoped HTSC are due to strong fluctuations of the superconducting order parameter (and in particular of its phase), which in turn would be due to either a Bose-Einstein-like preformation of Cooper pairs,[15] stripelike inhomogeneities,[14,17] or bidimensionality effects.[16] For instance, in Ref. 15, it is claimed that the superconducting fluctuations in underdoped HTSC will be given essentially by the 2D-Kosterlitz-Thouless model of fluctuations[45] with relaxation times of such fluctuations various orders of magnitude bigger than the BCS mean-field one implied by Eq. (8). However, our present analyses strongly suggest that there is no change in the order of magnitude of the superconducting fluctuations when the doping level enters the underdoped range. There is also no evidence in our experimental data of any dependence on x of the critical exponents of $\Delta\sigma_{ab}(\varepsilon)$ for $0.10 \leqslant x \leqslant 0.15$. Our results favor, then, the theoretical proposals associating the pseudogap opening with purely normal-state effects (as, e.g., those of Refs. 18–20), or the theories where the Bose-Einstein preformed pairs are dressed by normal quasiparticles.[21] In those

approaches, consistent with our present results, the superconducting order parameter is expected to undergo Gaussian, mean-field-like fluctuations, except in the very close vicinity of T_c (for $\varepsilon \lesssim 10^{-2}$). It would be useful to determine whether other proposals for the doping effects in HTSC, such as the existence of a $T=0$ K quantum transition near optimal doping,[46] would lead to Gaussian or non-Gaussian superconducting fluctuations above T_c.

The results presented here may also have implications on the theoretical proposals by Horbach *et al.*[47] for the paraconductivity in the marginal-Fermi-liquid scenario, which would apply to optimally doped and overdoped HTSC. According to the calculations in Ref. 47, the inelastic scattering of normal quasiparticles in optimally doped and overdoped HTSC would decrease the relaxation time of the superconducting fluctuations below the BCS mean-field value, and correspondingly also decrease $\Delta\sigma_{ab}$. Horbach *et al.* estimate such changes in $\Delta\sigma_{ab}$ to be of the order of a prefactor 0.2–0.75 (depending mainly on a cut parameter affecting their numerical evaluations).[47] However, our present results indicate that the relaxation time of the superconducting fluctuations takes the BCS mean-field value for all the doping levels. They also indicate that $\Delta\sigma_{ab}$ is not smaller in the optimally doped and overdoped films than it is in the underdoped films [in fact, it is even higher in the overdoped films because of their lower $\xi_c(0)$].

It may also be useful to compare our results for the $\xi_c(0)$ dependence on doping with detailed measurements of the normal-state anisotropy in LSCO films. For instance, in Ref. 48, the resistivity in LSCO thin films grown with the *c* axis oriented obliquely with respect to the substrate is measured. From such measurements, it was proposed that the normal-state anisotropy decreases as doping increases. If confirmed by different measurements, this would indicate that the interlayer tunneling of the normal and superconducting carriers are not directly related. This could be coherent, e.g., with the interlayer tunneling model for the superconducting condensation in HTSC proposed by Anderson *et al.*[20] Further work to compare the normal and superconducting interlayer tunnelings in LSCO films is clearly needed, both theoretical and experimental (for instance, through measurements of the intrinsic interlayer Josephson effects and of the normal and superconducting magnetoconductivity).

Further work is also needed to study the possible influence on the ''fine'' details of the superconducting fluctuations of the film thickness and of the type of substrate. As mentioned previously, both factors are known to vary several crucial properties of the LSCO films, such as their T_c and $\rho_{ab}(250\ \mathrm{K})$ values, possibly due in part to strain effects associated with the growth on a substrate with ab-plane lattice constants different to those of bulk LSCO.[1,4,7,22–26] In the present paper we have found a transversal superconducting coherence length for LSCO films which is different, both in value and doping dependence, to that which seems to arise from Ref. 40 (where the fluctuation magnetization in a bulk underdoped LSCO was measured) and Refs. 41,42 (where the superconducting anisotropy of LSCO bulk samples with different dopings was measured). It would be interesting, therefore, to study further the relationships between sample thickness, type of substrate, and superconducting interlayer tunnelings [or, equivalently, $\xi_c(0)$].

ACKNOWLEDGMENTS

This work was supported by the CICYT, Spain, under Grant Nos. MAT2001-3272 and MAT2001-3053, by the Xunta de Galicia under Grant No. PGIDT01PXI20609PR, and by Unión Fenosa under Grant No. 220/0085-2002.

*Present address: Low Temperature Division, Department of Applied Physics and MESA+ Research Institute, University of Twente, P.O. Box 217, 7500 AE Enschede, The Netherlands.

†Present address: Institute for Materials Research, Limburgs Universitair Centrum, Wetenschapspark 1, B-3590 Diepenbeek, Belgium.

‡Corresponding author. Email address: fmvidal@usc.es

§Unidad Asociada al Instituto de Ciencias de Materiales de Madrid, Consejo Superior de Investigaciones Científicas, Spain.

[1] For a detailed review of the doping effects in cuprates see, e.g., T. Timusk and B. Statt, Rep. Prog. Phys. **62**, 61 (1999); see also, V.M. Loktev, R.M. Quick, and S.G. Sharapov, Phys. Rep. **349**, 1 (2001); for a summary centered on LSCO, see, e.g., P.G. Radaelli, D.G. Hinks, A.W. Mitchell, B.A. Hunter, J.L. Wagner, B. Dabrowski, K.G. Vandervoort, H.K. Viswanathan, and J.D. Jorgensen, Phys. Rev. B **49**, 4163 (1994).

[2] The general aspects of the superconducting fluctuations in low- and high-T_c superconductors may be seen, e.g., in M. Tinkham, *Introduction to Superconductivity* (McGraw-Hill, New York, 1996), Ch. 8; W.J. Skocpol and M. Tinkham, Rep. Prog. Phys. **38**, 1049 (1975).

[3] For a summary of the paraconductivity in optimally doped HTSC and earlier references see, e.g., F. Vidal and M. V. Ramallo, in *The Gap Symmetry and Fluctuations in High-T_c Superconductors*, Vol. 371 of NATO Advanced Study Institute, Series B: Physics, edited by J. Bok, G. Deutscher, D. Pavuna, and S. A. Wolf (Plenum, New York, 1998), p. 443.

[4] M. Suzuki and M. Hikita, Phys. Rev. B **44**, 249 (1991); **47**, 2913 (1993).

[5] J.R. Cooper, S.D. Obertelli, A. Carrington, and J.W. Loram, Phys. Rev. B **44**, 12 086 (1991); A. Carrington, D.J.C. Walker, A.P. Mackenzie, and J.R. Cooper, *ibid.* **48**, 13 051 (1993).

[6] N. Mori, Y. Takano, H. Enomoto, H. Ozaki, and K. Sekizawa, Physica B **194–196**, 2049 (1994).

[7] T. Kimura, S. Miyasaka, H. Takagi, K. Tamasaku, H. Eisaki, S. Uchida, K. Kitazawa, M. Hiroi, M. Sera, and N. Kobayashi, Phys. Rev. B **53**, 8733 (1996).

[8] J.Y. Juang, M.C. Hsieh, C.W. Luo, T.M. Uen, K.H. Wu, and Y.S. Gou, Physica C **329**, 45 (2000).

[9] K. Asaka, K. Koizumi, H. Bando, N. Mori, and H. Ozaki, Physica

B **284–288**, 995 (2000).
[10] E. Silva, S. Sarti, R. Fastampa, and M. Giura, Phys. Rev. B **64**, 144508 (2001).
[11] A. Gueffaf, M. Salim, and M.S. Raven, J. Phys.: Condens. Matter **13**, 875 (2001).
[12] C. Meingast, V. Pasler, P. Nagel, A. Rykov, S. Tajima, and P. Olsson, Phys. Rev. Lett. **86**, 1606 (2001).
[13] B. Leridon, A. Défossez, J. Dumont, J. Lesueur, and J.P. Contour, Phys. Rev. Lett. **87**, 197007 (2001); **90**, 179704 (2003); C.W. Luo, J.Y. Juang, J.-Y. Lin, K.H. Wu, T.M. Uen, and Y.S. Gou, *ibid.* **90**, 179703 (2003).
[14] P. Carretta, A. Lascialfari, A. Rigamonti, A. Rosso, and A. Varlamov, Phys. Rev. B **61**, 12 420 (2000); A. Lascialfari, A. Rigamonti, L. Romano, P. Tedesco, A. Varlamov, and D. Embriaco, *ibid.* **65**, 144523 (2002).
[15] C.A.R. Sá de Melo, M. Randeria, and J.R. Engelbrecht, Phys. Rev. Lett. **71**, 3202 (1993); see also M. Randeria, in *Bose-Einstein Condensation*, edited by A. Griffin, D.W. Snoke, and S. Stringari (Cambridge University Press, Cambridge, 1995), and references therein.
[16] V.J. Emery and S.A. Kivelson, Nature (London) **374**, 434 (1995).
[17] B. Batlogg and V.J. Emery, Nature (London) **382**, 20 (1996).
[18] J. Schmalian, D. Pines, and B. Stojković, Phys. Rev. B **60**, 667 (1999).
[19] J. Bouvier and J. Bok, in *The Gap Symmetry and Fluctuations in High-T_c Superconductors*, Vol. 371 of NATO Advanced Series Institute, Series B: Physics, edited by J. Bok, G. Deutscher, D. Pavuna, and S. A. Wolf (Plenum, New York, 1998), p. 37.
[20] P.W. Anderson, *The Theory of Superconductivity in the High-T_c Cuprates* (Princeton University Press, Princeton, 1997), and references therein.
[21] V.B. Geshkenbein, L.B. Ioffe, and A.I. Larkin, Phys. Rev. B **55**, 3173 (1997).
[22] X.J. Chen, H. Q Lin, and C.D. Gong, Phys. Rev. B **61**, 9782 (2000).
[23] J.-P. Locquet, Y. Jaccard, A. Cretton, E.J. Williams, F. Arrouy, E. Mächler, T. Schneider, Ø. Fischer, and P. Martinoli, Phys. Rev. B **54**, 7481 (1996).
[24] H. Sato and M. Naito, Physica C **274**, 221 (1997); H. Sato, A. Tsukada, M. Naito, and A. Matsuda, Phys. Rev. B **61**, 12 447 (2000).
[25] I. Bozovic, G. Logvenov, I. Belca, B. Narimbetov, and I. Sveklo, Phys. Rev. Lett. **89**, 107001 (2002).
[26] H.L. Kao, J. Kwo, R.M. Fleming, M. Hong, and J.P. Manaerts, Appl. Phys. Lett. **59**, 2748 (1991).
[27] For a review of the influence of the inhomogeneities in the measurements of superconducting fluctuations, see F. Vidal, J.A. Veira, J. Maza, J. Mosqueira, and C. Carballeira, in *Materials Science, Fundamental Properties and Future Electronic Applications of High-T_c Superconductors*, edited by S.L. Drechsler and T.M. Mishonov (Kluwer, Dordrecht, 2001), p. 289. See also the references therein.
[28] J.A. Veira and F. Vidal, Phys. Rev. B **42**, R8748 (1990).
[29] M.V. Ramallo, A. Pomar, and F. Vidal, Phys. Rev. B **54**, 4341 (1996), and references therein; see also, M.V. Ramallo and F. Vidal, *ibid.* **59**, 4475 (1999).
[30] S.K. Yip, Phys. Rev. B **41**, 2612 (1990).
[31] M.T. Béal-Monod and K. Maki, Europhys. Lett. **33**, 309 (1996).
[32] C. Carballeira, S.R. Currás, J. Viña, J.A. Veira, M.V. Ramallo, and F. Vidal, Phys. Rev. B **63**, 144515 (2001).
[33] J. Viña, J.A. Campá, C. Carballeira, S.R. Currás, A. Maignan, M.V. Ramallo, I. Rasines, J.A. Veira, P. Wagner, and F. Vidal, Phys. Rev. B **65**, 212509 (2002).
[34] F. Vidal, C. Carballeira, S.R. Currás, J. Mosqueira, M.V. Ramallo, J.A. Veira, and J. Viña, Europhys. Lett. **59**, 754 (2002). A natural extension of the ideas summarized in this reference is provided by the superconducting fluctuations in the so-called high reduced-magnetic field regime, when $h \equiv H/H_{c2}(0)$ becomes of the order of unity, where H is the applied magnetic field and $H_{c2}(0)$ the upper critical field GL amplitude. In this case, the characteristic length of the superconducting wave function becomes of the order of the so-called magnetic length, $\ell_H = \xi(0)h^{-1/2}$. Therefore, the decrease of ℓ_H as h increases will also be bound by the limitations imposed by the uncertainty principle on the shrinkage of the superconducting wave function, i.e., by the condition $\ell_H \gtrsim \tilde{c}\xi_0$, where $\tilde{c}$ will be a cutoff constant of the order of unity. This directly leads to a reduced magnetic field h^c given by $\ell_H(h^c) = \tilde{c}\xi_0$, above which *all* superconducting fluctuations vanish. In the clean BCS limit $\xi(0) = 0.74\xi_0$ and therefore $h^c \simeq 0.6/\tilde{c}^2$.
[35] A. Gauzzi and D. Pavuna, Phys. Rev. B **51**, 15 420 (1995).
[36] Expressions for the Levanyuk-Ginzburg reduced temperature $\varepsilon_{\mathrm{LG}}$ in layered superconductors were calculated in M.V. Ramallo and F. Vidal, Europhys. Lett. **39**, 177 (1997); due to the ambiguities in the background subtraction and in the T_c determination, to discriminate between the 3DXY and GGL behaviors in the paraconductivity data, it is necessary to supplement their analysis with those of other superconducting fluctuation-induced observables. This was made for the case of the optimally doped YBCO by Ramallo *et al.* in Ref. 29. These analyses of high-quality data obtained in single crystals, not appreciably affected by stoichiometric and structural inhomogeneities, confirmed that in the $\varepsilon \gtrsim 10^{-2}$ region, the superconducting fluctuations behave as mean field like, whereas for $\varepsilon \lesssim 10^{-2}$ they follow the 3DXY predictions, in agreement then with the estimates based on the Levanyuk-Ginzburg criterion [see also M.V. Ramallo, C. Carballeira, and F. Vidal, Physica C **341–348**, 173 (2000)].
[37] J. Mosqueira, C. Carballeira, and F. Vidal, Phys. Rev. Lett. **87**, 167009 (2001).
[38] In fact, this estimate is expected to be roughly correct also in moderately dirty BCS superconductors (when $\ell \lesssim \xi_0$, ℓ being the mean free path of the normal carriers) because both the GL coherence length amplitude and the actual superconducting coherence length at $T = 0$ K will be affected by impurities to a similar extent [see, e. g., P. G. de Gennes, *Superconductivity of Metals and Alloys* (W. A. Benjamin, New York, 1966), Sec. 7.2].
[39] M.V. Ramallo, C. Carballeira, J. Viña, J.A. Veira, T. Mishonov, D. Pavuna, and F. Vidal, Europhys. Lett. **48**, 79 (1999).
[40] C. Carballeira, J. Mosqueira, A. Revcolevschi, and F. Vidal, Phys. Rev. Lett. **84**, 3157 (2000); Physica C **384**, 185 (2003).
[41] Y. Nakamura and S. Uchida, Phys. Rev. B **46**, 5841 (1992).
[42] T. Shibauchi, H. Kitano, K. Uchinokura, A. Maeda, T. Kimura, and K. Kishio, Phys. Rev. Lett. **72**, 2263 (1994).
[43] B. Oh, K. Char, A.D. Kent, M. Naito, M.R. Beasley, T.H. Geballe, R.H. Hammond, A. Kapitulnik, and J.M. Graybeal, Phys. Rev. B **37**, 7861 (1988).
[44] J.A. Veira and F. Vidal, Physica C **159**, 468 (1989).
[45] J.M. Kosterlitz and D.J. Thouless, J. Phys. C **6**, 1181 (1973).

[46] See, e.g., C.M. Varma, Phys. Rev. Lett. **83**, 3538 (1999); see also, C. Panagopoulos, J.L. Tallon, B.D. Rainford, T. Xiang, J.R. Cooper, and C.A. Scott, Phys. Rev. B **66**, 064501 (2002), and references therein.

[47] M.L. Horbach, F.L.J. Vos, and W. van Saarloos, Phys. Rev. B **49**, 3539 (1994).

[48] H.L. Kao, J. Kwo, H. Takagi, and B. Batlogg, Phys. Rev. B **48**, 9925 (1993).